Effects of composition fluctuations on the structure and development of laminar and turbulent flame kernels

Aimad Er-raiy, Zakaria Bouali, Arnaud Mura
Institut Pprime - UPR 3346 - CNRS - ENSMA - Université de Poitiers
BP 40109, 86961 Futuroscope, France

1 Introduction

Propagation of turbulent flames in a non-homogeneous mixture of reactants has a large number of practical applications including those relying on constant-volume combustion cycles. The corresponding hetererogeneities concern both temperature and equivalence ratio, which may result from several distinct factors such as the presence of residual burnt gases issued from the previous cycle, i.e., exhaust gases recirculation (EGR), the internal flowfield or the preliminary dispersion and evaporation of a spray of liquid droplets. The present work aims at investigating some of the effects that may result from the joint influence of turbulence and mixture heterogeneities on the flame propagation. It is quite clear that the resulting flames (i) have a more complex structure than fully-premixed or diffusion turbulent flames and (ii) still remain neither perfectly understood nor mastered. Since the early investigations conducted by Ishikawa [1] significant improvements have been made in the application of measurement techniques and diagnostics and some experimental databases that address combustion in heterogeneous environments are now available [2, 3] but they are still relatively scarce. From the numerical point of view, the use of direct numerical simulation (DNS) has been early considered [4] and recently generalized, mainly, to explore the effects of equivalence ratio heterogeneities on flame propagation [5–7]. However, with only a few exceptions (see for instance [8–10]), most of the previous analyses were conducted under the single-step chemistry simplification. The present work thus aims at complementing some of these previous investigations, which were focused on the smallest scales features in such inhomogeneous conditions, through the analysis of a new DNS dataset, which relies on a representative chemical scheme featuring 29 chemical species and 48 elementary reaction steps.

2 Numerical methods and initial conditions

The present computations are performed with the dilatable low-Mach number DNS solver *Asphodele* [9–11]. Spatial derivatives are evaluated with a fourth order finite difference scheme while time integration is performed with a low-storage third-order Runge-Kutta scheme. Iso-octane chemistry is described with the mechanism developed by Hasse et al. [12]. This fuel is known to be hardly involved in auto-ignition processes and this allows to focus on flame-propagation phenomena. The Hasse's mechanism has been widely validated against experiments over a rather large range of operating conditions in terms of temperature, pressure, equivalence ratio and dilution variations. The main goal of the present study is to quantify the impact of temperature and equivalence ratio heterogeneities on the flame propagation period that follows the ignition step. Therefore, ignition phenomena are dismissed and a perfectly-ignited flame kernel is initialized in the center of the computational domain. The corresponding species mass fractions and temperature profiles are deduced from the preliminary computation

Correspondence to: aimad.er-raiy@ensma.fr

of a one-dimensional laminar unstrained premixed flame performed with *Cantera* [13]. The development of the kernel is then studied in decaying homogeneous isotropic turbulence (HIT) in the presence of temperature or equivalence ratio heterogeneities. The initial fluctuating velocity field is generated on the basis of the classical Rogallo's procedure according to a Passot-Pouquet spectrum. Due to the high CPU costs of DNS conducted with skeletal chemistry mechanisms, only two-dimensional configurations are considered below. The simulation domain corresponds to a square domain of dimension $L_x = L_y = 4\,mm$. The temperature and equivalence ratio scalar fields $\xi(\boldsymbol{x}, t = 0)$ are initialized using the spectral procedure described by Reveillon [14] with a prescribed level of fluctuations (i.e., variance $\widetilde{\xi''^2}$) and a characteristic size l_ξ. This method allows to generate isotropic fluctuating scalar fields for various values of the segregation-rate and characteristic length scale l_ξ. With the objective of being able to discriminate the influence of the heterogeneities from the effects of turbulence, the present set of DNS data gathers both laminar and turbulent conditions. The analyses are focused on the impact of the (i) type of heterogeneity (temperature or equivalence ratio), (ii) segregation-rate value, i.e., $S_\xi = \widetilde{\xi''^2}/\widetilde{\xi}(1-\widetilde{\xi})$ for a scalar bounded between zero and unity, and (iii) characteristic size l_ξ. Two distinct values are considered for the last two parameters and the initial segregation-rate level is either considered as moderate ($S_\xi = 0.4$) or large ($S_\xi = 0.8$), while the characteristic length scale is set to either $l_\xi = L_x/10$ or $L_x/4$.

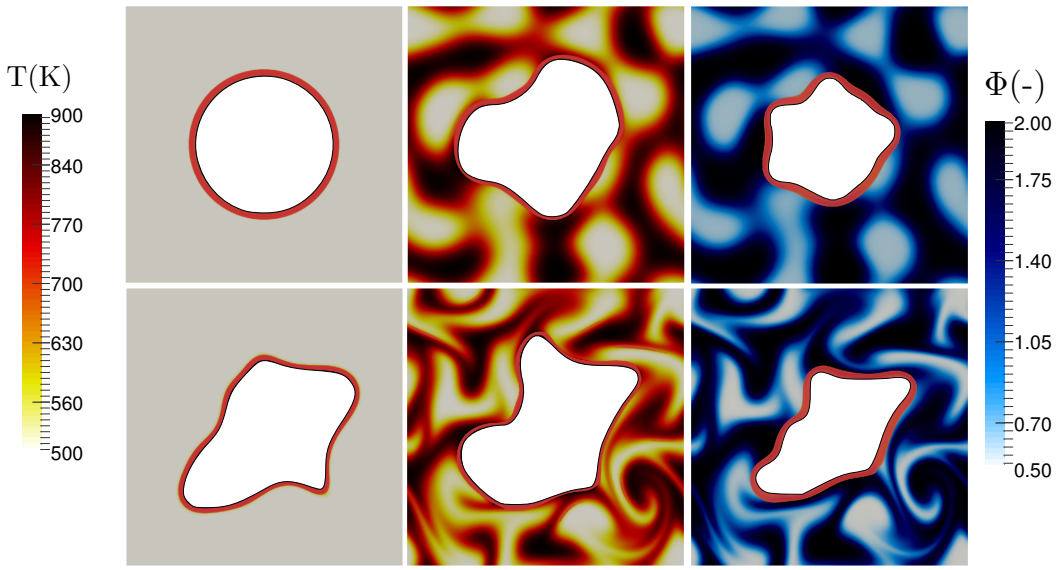

Figure 1: DNS results obtained at $t = 4\tau_L^0$. Left to right: homogeneous fresh reactants, temperature heterogeneities, and equivalence-ratio heterogeneities, laminar (top) versus turbulent (bottom) cases.

The initial ambient pressure and temperature are respectively set to $5\ bar$ and $700K$, respectively. Two global equivalence ratios were considered: lean ($\overline{\Phi} = 0.7$) and stoichiometric ($\overline{\Phi} = 1.0$). The values of the laminar flame speed S_L^0 is equal to $0.65\,m.s^{-1}$ (resp. $1.22\,m.s^{-1}$) for $\Phi = 0.7$ (resp. $\Phi = 1$). The laminar flame thickness δ_L^0 corresponds to $112\,\mu m$ (i.e, approximately 1/35 times the domain size L_x) for $\Phi = 0.7$ and it is $78\,\mu m$ (i.e, approximately 1/50 times the domain size L_x) for $\Phi = 1$. In turbulent cases, the integral length scale is set to $l_T = 0.5\,mm$ (i.e, approximately 8 times the domain size L_x) and the initial root mean square (RMS) of velocity fluctuations is set to $u_{\text{RMS}} = 1.2\,m.s^{-1}$ leading to a value of fifty for the turbulent Reynolds number Re_T.

2 Direct numerical simulation results

Figure 1 illustrates some results that are extracted from this new set of DNS databases. The fields that are displayed on the left of Fig.1 correspond to the reference case of a flame propagating in a homogeneous stoichiometric mixture, the flow regime is laminar on the top and turbulent on the bottom. In contrast to the reference case, some distortion of the flame front are observed in the presence of either temperature or equivalence-ratio heterogeneities. Special attention is first paid to laminar cases. As far as temperature heterogeneities are concerned, chemical reaction is favored in the vicinity of hot pockets, which leads to flame wrinkling and accelerates also the whole propagation of the flame front. This behavior is quantitatively assessed in Fig.2, which reports the evolutions of the equivalent radius of the flame front (left side of Fig.2) together with the heat release rate $\dot{\omega}_{\text{HRR}}$, which is integrated over the entire computational domain and normalized by its initial value $\dot{\omega}_{\text{HRR}}^{t_0}$. The two quantities are reported as functions of the non-dimensional time t/τ_L^0, with $\tau_L^0 = \delta_L^0/S_L^0$ the transit time across the laminar premixed flame of reference.

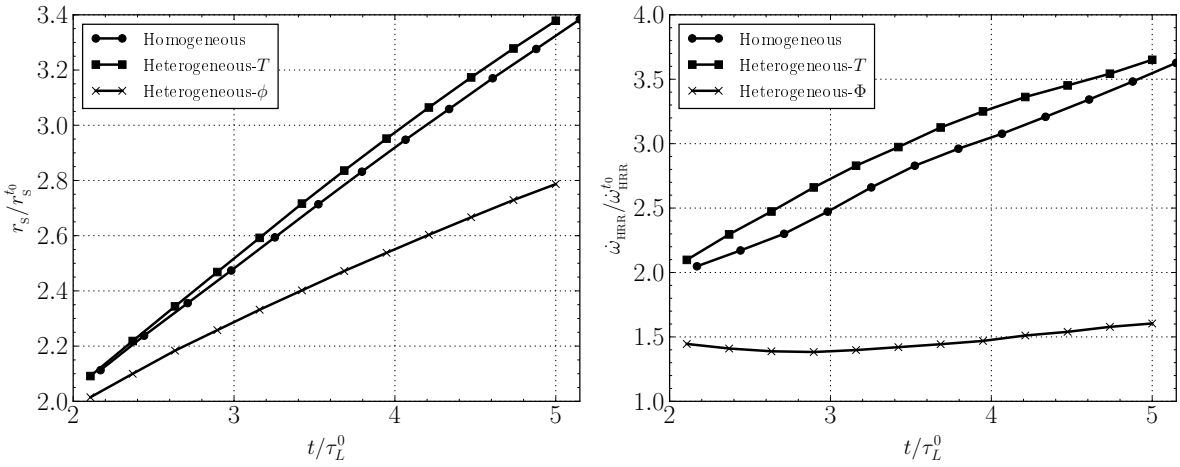

Figure 2: Temporal evolutions of the normalized flame equivalent radius $r_s/r_s^{t_0}$ with $r_s^{t_0}$ the initial kernel radius (left) and normalized global heat release rate $\dot{\omega}_{\text{HRR}}/\dot{\omega}_{\text{HRR}}^{t_0}$ (right).

Concerning the influence of equivalence ratio heterogeneities, it appears that, for the present conditions, the overall propagation of the laminar flame is slower compared to the stoichiometric reference case. This is an outcome of the laminar flame velocity dependency to the equivalence ratio, which displays a bell-shaped profile: the propagation velocity reaches it maximum value in the vicinity of stoichiometry and decays as the equivalence ratio is either increased towards rich mixtures or decreased towards lean mixtures. The presence of either rich or lean zones around the stoichiometry thus tends to slow down the overall propagation as highlighted in Fig.2. It is noteworthy that this specific conclusion is altered for lean conditions ($\overline{\Phi} = 0.7$). The wrinkling of the flame front in presence of equivalence ratio heterogeneities is also found to be less important compared to the case featuring temperature heterogeneities. In fact, the laminar flame propagation velocity does indeed not only display an important sensitivity to the equivalence ratio Φ but also to the unburnt mixture temperature T_0, i.e., $S_L^0 = S_L^0(\Phi, T_0)$, and it can be shown that the magnitude of the fluctuations of S_L^0 associated to the initial temperature distribution is more important than the one issued from equivalence ratio variations. This influence of composition heterogeneities persists in turbulent conditions. The curvature probability density functions (PDF) are indeed wider in the presence of either temperature or equivalence ratio heterogeneities, see Fig.3, and similar effects are also visible on the strain-rate PDFs, see Fig.4. The above results confirm the relevance of studying the influence of heterogeneities in laminar conditions to get a better understanding of the

related phenomena in turbulent reactive flow conditions.

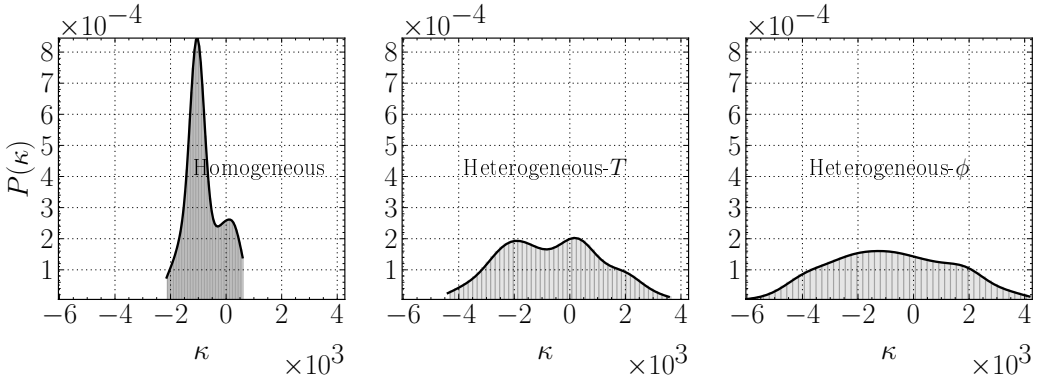

Figure 3: PDFs of the curvature of the flame surface for the three turbulent cases.

We will now proceed with additional standard post-processing procedures applied to turbulent cases, which can be classified into two categories (i) geometric examination and (ii) turbulent mixing analyses.

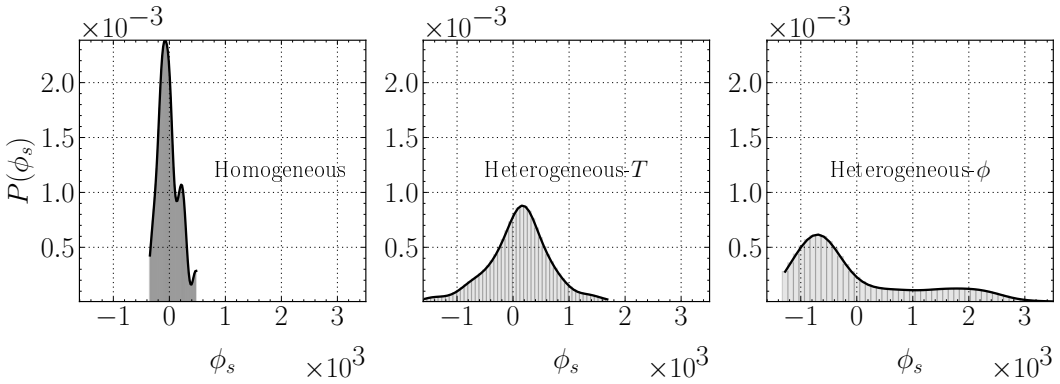

Figure 4: PDFs of the in-plane strain-rate that applies on the flame surface for the three turbulent cases.

2.1 Geometric framework

The flame front is considered as a thin propagative interface separating the fresh reactants from the burned products. The turbulent flame is analyzed in terms of averaged flame surface density (FSD) evaluation, local flame displacement speed determination, strain-rate and curvature PDFs. Considering a semi-detailed chemical scheme there exist several relevant definitions for the progress variable, which can be based for instance on a normalized combination of species mass fractions or on a normalized temperature $c_T(\boldsymbol{x},t) = (T(\boldsymbol{x},t) - T_u(\boldsymbol{x},t))/(T_b(\boldsymbol{x},t) - T_u(\boldsymbol{x},t))$, where the burned gases temperature $T_b(\boldsymbol{x},t)$ will depend on the initial values of both equivalence ratio (or mixture fraction) and temperature. Several other definitions have been considered within the course of the present analysis. For instance, we also considered (i) a definition based on the normalized sum of the CO and CO_2 mass fractions, i.e., $(Y_{\mathrm{CO}} + Y_{\mathrm{CO_2}})/(Y^{eq}_{\mathrm{CO}} + Y^{eq}_{\mathrm{CO_2}})$, as well as a definition based on the normalized specific volume $\mathcal{V} = 1/\rho$ [15]. However, unless otherwise stated, the results reported herein are based on the normalized temperature. Normal directions to flame surface are thus defined as the normalized gradient of the progress variable: $\boldsymbol{n_c} = -\boldsymbol{\nabla} c/\|\boldsymbol{\nabla} c\|$, which allows to define the flame curvature as $\kappa = -\boldsymbol{\nabla}\cdot\boldsymbol{n_c}$. The total flame stretch φ, i.e., the normalized rate of variation of the flame surface, is subsequently analyzed as the sum of two distinct contributions: (i) curvature-propagation effects and (ii) in-plane strain-rate ϕ_s

$$\varphi = S_d\boldsymbol{\nabla}\cdot\boldsymbol{n_c} + \phi_s = S_d\boldsymbol{\nabla}\cdot\boldsymbol{n_c} + (\boldsymbol{\nabla}\boldsymbol{u} - \boldsymbol{n_c}\boldsymbol{n_c} : \boldsymbol{\nabla}\boldsymbol{u}) \tag{1}$$

where S_d denotes the flame front displacement and $\boldsymbol{n_c}\boldsymbol{n_c} : \boldsymbol{\nabla}\boldsymbol{u}$ is equivalent to $\boldsymbol{n_c}\cdot(\boldsymbol{n_c}\cdot\boldsymbol{\nabla})\boldsymbol{u}$. Finally, the mean FSD has been evaluated as either the conditional average of the progress variable gradient

through the flame $\langle \Sigma(c^*,t)\rangle = \langle \|\nabla c(\boldsymbol{x},t)\|\ \delta(c(\boldsymbol{x},t)-c^*)\rangle$ and compared to the generalized FSD $\langle\Sigma\rangle = \langle\|\nabla c(\boldsymbol{x},t)\|\rangle$.

2.2 Turbulent mixing description

The mean FSD discused above is closely related to the local gradient of the progress variable and, in practice, the modelling of turbulent premixed flames requires information on the scalar gradient in one form or another. For instance, presumed or transported probability density function (PDF) frameworks require a closure for the average or conditional scalar dissipation rate (SDR) $N_c = D(\partial c/\partial x_i)\cdot(\partial c/\partial x_i)$ to be settled. In recent years special attention has been paid to the turbulence-scalar interaction (TSI) term, which plays an essential role in the SDR budget [6]

$$\mathrm{TSI} = -2\overline{\rho N_c^{ij}\partial u_j/\partial x_i} = -2\overline{\rho N_c \sum_{k=1}^{k=2}\lambda_k \cos^2(\theta_k)} \tag{2}$$

with $N_c^{ij} = D\cdot(\partial c/\partial x_i)\cdot(\partial c/\partial x_j)$ the SDR tensor. The quantities λ_i denote the eigenvalues of the strain-rate tensor $S_{ij} = (\partial u_i/\partial x_j + \partial u_j/\partial x_i)/2$. Since S_{ij} is a symmetric second rank tensor, they are real numbers, ordered by $\lambda_1 > \lambda_2$, where $\lambda_1 > 0$ represents the most extensive principal direction and $\lambda_2 < 0$ corresponds to the most compressive principal direction. It is important to notice that the intermediate eigenvalue, which reflects the intensity of turbulent transfer in a three-dimensional turbulent flow is discarded from the present two-dimensional analysis. The TSI term reflects the production (or dissipation) of scalar gradients by the action of turbulence and the production of scalar gradients will result from a preferential alignment of the scalar gradient with the principal direction of compression.

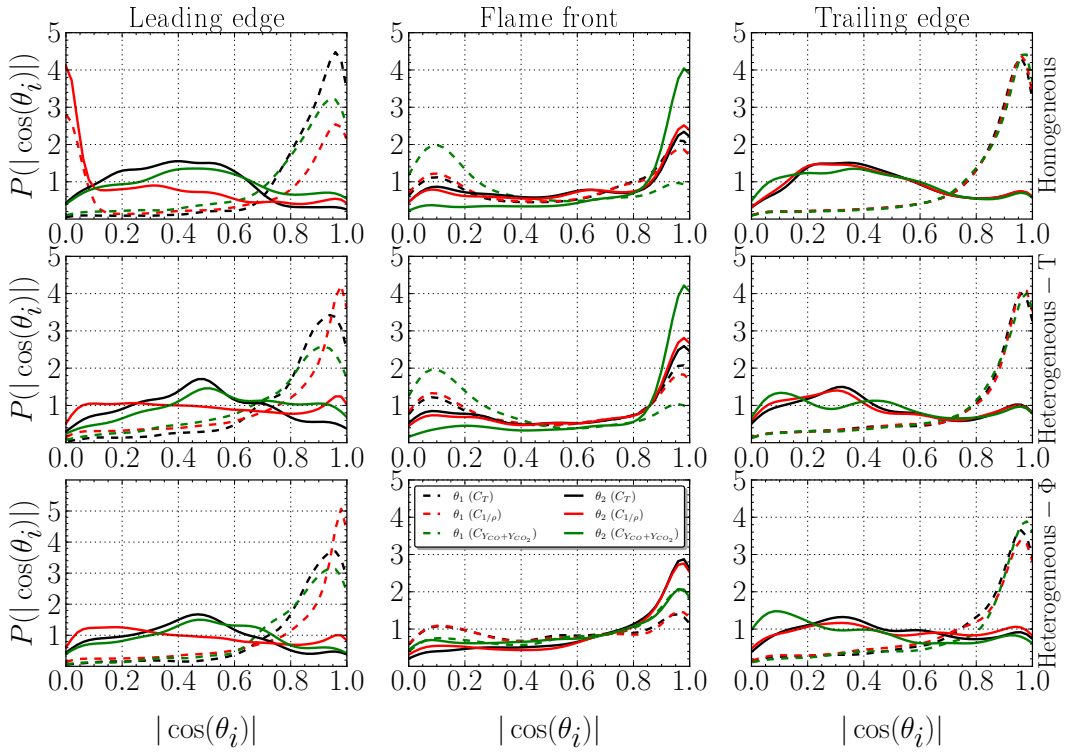

Figure 5: Statistics of the alignement between $\boldsymbol{n_c}$ and the eigenvectors of the strain-rate tensor using three distinct definitions of the progress variable.

Alignment statistics between strain-rate principal directions and scalar gradients are reported in Fig. 5. The reactive flowfields are analyzed in three regions: the leading edge ($0.001 < c < 0.05$), the flame

front ($0.05 < c < 0.95$), and the trailing edge ($0.95 < c < 0.999$). The analysis of the present set of DNS data suggests that scalar gradient is produced through the TSI term far from the flame (on either the leading or trailing edge), while it is decreased across the flame front. Far from the flame, the turbulent processes tend to bring isoscalar surfaces together: the normal direction $\boldsymbol{n_c}$ tends to be aligned with the most compressive principal direction of the strain-rate tensor, leading to scalar gradient production. Across the flame front, the dilatation induced by the heat release overhelms the effects of turbulence and the scalar gradient preferentially aligns with the most extensive strain rate. The observed trends thus confirms previous studies of Malkeson and Chakraborty [6]. However, it is noteworthy that the obtained results display a non-negligible sensitivity to the choice and definition of the retained progress variable.

3 Conclusions and perspectives

A new set of DNS databases is generated to investigate the influence of temperature and composition heterogeneities on flame propagation. Both laminar and turbulent cases are analysed. The focus is placed on flame-propagation phenomena and a realistic description of chemistry of iso-octane in air has been considered. Despite some sensitivity to the choice of the retained progress variable, the present confirms some of the trends that were highlighted in previous analyses of DNS databases based on a single-step global chemistry. However, as the mean equivalence ratio is varied, some differences - which are not reported here just for the sake of conciseness - are also found.

Acknowledgements: this work is a part of the PhD. Thesis of A. Er-Raiy supported by the CAPA Program (CNRS, ENSMA, SAFRAN and MBDA) of the ANR (Agence Nationale de la Recherche).

References

[1] Ishikawa N. (1983). Combustion of stratified methane-air layers. Combust. Sci. Tech., 30:311-325

[2] Robin V., Mura A., Champion M., Degardin O., Renou B., Boukhalfa M. (2008), Experimental and numerical analysis of stratified turbulent V-shaped flames, Combust. Flame, 153:288-315

[3] Kamal M., Barlow R.S., Hochgreb S. (2015), Conditional analysis of turbulent premixed and stratified flames on local equivalence ratio and progress of reaction, Combust. Flame, 162:3896-3913

[4] Hélie J., Trouvé A. (1998), Turbulent flame propagation in partially premixed combustion, Proc. Combust. Inst., 27:891-898

[5] Chakraborty N., Mastorakos E., Cant R.S. (2007), Effects of turbulence on spark ignition in inhomogeneous mixtures: a direct numerical simulation (DNS) study, Combust. Sci. Tech., 179:293-317

[6] Malkeson S.P., Chakraborty N. (2011), Statistical analysis of scalar dissipation rate transport in turbulent partially premixed flames, Flow Turbul. Combust., 86:1-44

[7] Malkeson S. P., Chakraborty N. (2011). Statistical analysis of cross scalar dissipation rate transport in turbulent partially premixed flames, Flow Turbul. Combust., 87:313-349

[8] Jiménez C., Cuenot B., Poinsot T., Haworth D. (2002), Numerical simulation and modeling for lean stratified propane-air flames, Combust. Flame, 128:1-21

[9] Pera C., Chevillard S., Reveillon J. (2013), Effects of residual burnt gas heterogeneity on early flame propagation and cyclic variability in spark-ignited engines, Combust. Flame, 160:1020-1032

[10] Chevillard S., Michel J.B., Pera C., Reveillon J. (2017), Evaluation of turbulent combustion models based on tabulated chemistry, Combust. Theor. Modelling (in print).

[11] Bouali Z., Pera C., Reveillon J. (2012), Numerical analysis of the influence of two-phase flow mass and heat transfers on n-heptane autoignition, Combust. Flame, 159:2056-2068

[12] Hasse, C., Bollig, M., Peters, N., Dwyer, H. A. (2000). Quenching of laminar iso-octane flames at cold walls, Combust. Flame, 122:117-129

[13] Cantera, Chemical Kinetics, Thermodynamics, Transport Processes, http://www.cantera.org/ (accessed December 6, 2016)

[14] Reveillon J. (2005), Numerical procedures to generate and to visualize flow fields from analytical or experimental statistics, J. Flow Vis. Image Proc., 12:251-269

[15] Serra S., Robin V., Mura A., Champion M. (2014), Density variations effects in turbulent diffusion flames: modeling of unresolved fluxes, Combust. Sci. Tech., 186:1370-1391